



OIP5-AS1/miR-455-3p/microfibril-associated protein 2 axis exacerbates the progression of thyroid carcinoma

Rui Huang, Hongchun Liu, Changmin Wang

Center of Clinical Laboratory, People's Hospital of Xinjiang Uygur Autonomous Region, Urumqi, China

Contributions: (I) Conception and design: R Huang, C Wang; (II) Administrative support: H Liu; (III) Provision of study materials or patients: All authors; (VI) Collection and assembly of data: R Huang, H Liu; (V) Data analysis and interpretation: All authors; (VI) Manuscript writing: All authors; (VII) Final approval of manuscript: All authors.

Correspondence to: Changmin Wang, MS. Center of Clinical Laboratory, People's Hospital of Xinjiang Uygur Autonomous Region, No. 91 Tianche Road, Urumqi 830001, China. Email: wcm224@126.com.

Background: The long non-coding RNA (lncRNA) Opa interacting protein 5-antisense RNA 1 (OIP5-AS1) has been shown to participate in numerous biological and pathological processes, notably including oncogenesis. OIP5-AS1 modulates oncogenic or anti-tumor activities by controlling various microRNAs (miRs) in diverse cancer types. This study sought to examine the potential role of the lncRNA OIP5-AS1-mediated miR-455-3p/microfibril-associated protein 2 (MFAP2) axis and its influence on the progression of thyroid carcinoma.

Methods: Cell proliferation, migration, and apoptosis were assessed through *in vitro* experimental measurements, which involved the use of Cell Counting Kit 8 (CCK8), transwell, and terminal deoxynucleotidyl transferase-mediated dUTP nick-end labeling (TUNEL) staining techniques. The estimate algorithm was employed to examine the relationship between MFAP2 and the Stromal score, Immune score, and ESTIMATE score.

Results: OIP5-AS1 expression was significantly more elevated in the thyroid carcinoma tissues and cell lines than the corresponding normal non-tumor tissues and cell lines. Following transfection with short-hairpin (sh)-OIP5-AS1, the CAL62 and SW1736 cells upregulated miR-455-3p and downregulated the MFAP2 expression levels. The downregulation of OIP5-AS1 expedited cellular apoptosis and hindered cellular proliferation and migration in the CAL62 and SW1736 cells. The *in vitro* experiments showed that both the suppression of MFAP2 and the increased expression of miR-455-3p exerted significant anti-cancer effects. In addition, the overexpression of MFAP2 counteracted the *in vitro* antineoplastic effects of the sh-OIP5-AS1 and miR-455-3p mimics.

Conclusions: The results suggest that lncRNA OIP5-AS1 plays a crucial role in the advancement of thyroid carcinoma by inhibiting miR-455-3p to activate MFAP2.

Keywords: Long non-coding RNA (lncRNA); microfibril-associated protein 2 (MFAP2); anaplastic thyroid carcinoma; microRNA (miR); antineoplastic effects

Submitted Apr 17, 2024. Accepted for publication May 30, 2024. Published online Jun 27, 2024.

doi: 10.21037/tcr-24-630

View this article at: <https://dx.doi.org/10.21037/tcr-24-630>

Introduction

Microfibril-associated protein 2 (MFAP2), also referred to as MAGP1, is involved in cell adhesion, movement, and matrix modification through its extracellular and intracellular regions (1,2). MAGP1 deficiency (MFAP2^{-/-})

is associated with a range of metabolic disorders, including adipose accumulation, hyperglycemia, insulin resistance, dysangiogenesis, and cancellous and cortical bone loss (3-6), and evidence suggests that it may play a pathological role in these conditions. There is a growing body of research

that suggests that MAGP1 plays a center role in the advancement of cancerous growths (7-11). For instance, MFAP2 has been confirmed to be overexpressed in gastric cancer tissues, and MFAP2 has the ability to enhance cell proliferation, migration, invasion, and epithelial-mesenchymal transition (EMT), thereby worsening the progression of gastric cancer (7,8). MFAP2 has also been shown to facilitate liver cancer cell growth and can serve as a poor prognostic indicator (9). Similar pathological roles of MFAP2 have also been reported in breast cancer, melanoma, and papillary thyroid cancer (10,11). However, the roles of MFAP2 in human anaplastic thyroid carcinoma (thyroid carcinoma) are still unknown. Our results suggest that MFAP2 is upregulated in thyroid carcinoma tissues and plays a role in the malignant phenotypes of this type of cancer, including increased cell growth, migration, and infiltration. Further, our results also provide insights into the regulatory mechanism of MFAP2 in the advancement of thyroid carcinoma.

Long non-coding RNAs (lncRNAs) are closely associated with the development of cancer through the classical

regulatory mechanism of competing endogenous RNAs (ceRNAs), which act as sponges for microRNAs (miRs) to regulate downstream genes at the post-transcriptional level (12-14). In human thyroid carcinoma, numerous lncRNAs, including prostate cancer antigen 3, HOXA transcript antisense RNA myeloid-specific 1, papillary thyroid carcinoma susceptibility candidate 3, and metastasis associated lung adenocarcinoma transcript 1, play roles as either oncogenes or tumor suppressors (15-17). LncRNA Opa interacting protein 5-antisense RNA 1 (OIP5-AS1) is a notorious tumor-associated lncRNA that accelerates oncogenesis and tumor development (18). The high expression of OIP5-AS1 is closely associated with chemotherapy and radiotherapy resistance, as well as cancer metastasis and recurrence in humans (19-21). The increased expression of OIP5-AS1 enhances cellular growth and migration, and is indicative of an unfavorable prognosis in thyroid carcinoma (22). Our research confirmed that the expression of OIP5-AS1 was significantly more elevated in thyroid carcinoma samples than neighboring non-tumor tissues. Moreover, we also examined whether OIP5-AS1 had the ability to regulate the expression of MFAP2 in thyroid carcinoma. We used bioinformatics algorithms and experimental measurements to show that the progression of thyroid carcinoma worsened due to the obstruction of miR-455-3p-mediated MFAP2 repression by OIP5-AS1, which also revealed its function as a ceRNA. We present this article in accordance with the MDAR reporting checklist (available at <https://tcr.amegroups.com/article/view/10.21037/tcr-24-630/rc>).

Highlight box

Key findings

- Long non-coding RNA (lncRNA) Opa interacting protein 5-antisense RNA 1 (OIP5-AS1) plays a crucial role in the advancement of thyroid carcinoma by inhibiting microRNA-455-3p (miR-455-3p) to activate microfibril-associated protein 2 (MFAP2). Targeting MFAP2 could potentially improve the effectiveness of immunotherapy in thyroid carcinoma.

What is known and what is new?

- OIP5-AS1, a lncRNA regulated by methyltransferase-like14, is crucial in the progression of papillary thyroid cancer, and OIP5-AS1/miR-455-3p/MFAP2 signaling axis provides novel perspectives on the regulatory pathways involved in the development of this type of cancer.
- Our study revealed that the miR-455-3p/MFAP2 signaling axis plays a role in the advancement of thyroid cancer as a newly identified downstream regulatory pathway of OIP5-AS1. Additionally, MFAP2 may be linked to the infiltration of immune cells in thyroid cancer.

What is the implication, and what should change now?

- The findings indicate that OIP5-AS1 may play a role in the advancement of thyroid cancer via various signaling pathways, such as messenger RNA methylation and immunoinfiltration. These results offer a potential target for the development of combination therapy for thyroid cancer. Our initial assessment suggests that targeting MFAP2 could serve as a pathway to enhance the effectiveness of immunotherapy.

Methods

Clinical specimens

The study was approved by the Ethics Committee of the People's Hospital of Xinjiang Uygur Autonomous Region (approval number: 20210345). Informed consent forms were signed by the thyroid carcinoma patients before sample collection. In total, 13 thyroid carcinoma tissues and neighboring non-cancerous tissues were collected from patients at the People's Hospital of Xinjiang Uygur Autonomous Region. The study conformed to the provisions of the Declaration of Helsinki (as revised in 2013).

Cell cultures

The Nthy-ori3-1 cell line, as well as the SW1736 and CAL62 thyroid carcinoma cell lines, was acquired from the

American Type Culture Collection. These cell lines were cultured in Dulbecco's Modified Eagle Medium (Invitrogen, Thermo Fisher Scientific, MA, USA) supplemented with 10% fetal bovine serum. The cells were kept at a temperature of 37 °C in an environment containing 5% carbon dioxide and 95% ambient air. The cell experiment involved three biological replicates in each group.

Cell transfection

The MFAP2 short-hairpin (sh) RNA, miR-455-3p mimics, lncRNA OIP5-AS1 shRNA, and MFAP2 overexpressed plasmids were provided by Gene-Pharma (Shanghai, China). Cell transfection was performed using Lipofectamine 3000 (Invitrogen) in accordance with the manufacturer's instructions.

Histologic examination

The immunohistochemical (IHC) staining and histologic scoring processes were carried out as described previously (23,24). Anti-MFAP2 primary antibody (ab231627; dilution: 1:50; Abcam, Cambridge, United Kingdom) was used to incubate the histologic sections overnight at 4 °C. The tissue sections underwent treatment with a biotinylated anti-rabbit secondary antibody (Thermo Fisher Scientific, Waltham, MA, USA), subsequent incubation with the streptavidin-horseradish peroxidase complex (Thermo Fisher Scientific), immersion in 3,3'-diaminobenzidine, counterstaining with 10% Mayer's hematoxylin, dehydration, and mounting. The sections were evaluated based on the proportion of positively stained tumor cells, with scores ranging from 0 (no positive tumor cells) to 3 (>50% positive tumor cells). Staining intensity was graded on a scale from 0 (no staining) to 3 (strong staining). The staining index (SI) was determined by multiplying the staining intensity score by the proportion of positive tumor cells. We assessed expression of the MFAP2 in IHC-stained tumor sections based on the SI scores as 0, 1, 2, 3, 4, 6 and 9.

Western blot

The western blot procedures were performed as described previously (23,24). Anti-MFAP2 primary antibody (dilution: 1:1,000; Abcam), anti-β-actin primary antibody (cat. no. sc-130065; dilution: 1:2,000; Santa Cruz Biotechnology, DALLA, TX, USA), and secondary antibody goat anti-mouse IgG H&L horseradish peroxidase (cat. no: ab205719; dilution:

1:10,000; Abcam, Cambridge, United Kingdom) were used for the western blot analysis.

Reverse transcription quantitative polymerase chain reaction (RT-qPCR)

Total RNA was extracted using the miRNeasy Mini Kit (Qiagen, Inc., Valencia, CA, USA). The complementary DNA (cDNA) was synthesized using the first-strand cDNA synthesis kit (Takara Shuzo, Kyoto, Japan). TaqMan® Universal PCR Master Mix (Thermo Fisher Scientific, Inc., Waltham, MA, USA) was used for the PCR analysis. The following PCR primers were used: forward primer, 5'-GACCACGTCCAGTACACCC-3' and reverse primer, 5'-CCGAGGAGTCACCTCTTGATAA-3' for MFAP2; forward primer, 5'-ACACTCCAGCTGGGTAGCACC thyroid carcinoma TGAAT-3' and reverse primer, 5'-TGG TGTCGTGGAGTCG-3' for miR-455-3p; forward primer, 5'-GAAGATGGCGGAGTAAGGC-3' and reverse primer, 5'-AATGTTTCGGTTAGTTCCTCTCC-3' for OIP5-AS1; forward primer, 5'-GGAGCGAG thyroid carcinoma CCTCCAAAAT-3' and reverse primer, 5'-GGCTGTTGTCATACTTCTCATGG-3' for glyceraldehyde-3-phosphate dehydrogenase; forward primer, 5'-CTCGCTTCGGCAGCACA-3' and reverse primer, 5'-AACGCTTCACGAATTTGCGT-3' for U6 small nuclear RNA.

Cell proliferation, migration, invasion, and apoptosis

The Cell Counting Kit-8 (CCK-8) was obtained from the Beyotime Institute of Biotechnology (Haimen, China). Cells (5×10^3 /mL) were seeded into the wells of 96-well plates and incubated for 24 hours prior to transfection. Following transfection for 48 h, 10 μL of CCK8 reagent was added to each well and incubated at 37 °C for 1 hour. Cell viability in each well was assessed by measuring absorbance at 450 nm with a SpectraMax M5 ELISA plate reader (Molecular Devices, LLC, Sunnyvale, CA, USA).

The Transwell migration (without Matrigel) assay and Matrigel invasion assay (Corning Incorporated, Corning, NY, USA) were performed for migration and invasion, respectively. Cells that had migrated and invaded the bottom surface of the membrane were immobilized in 1% paraformaldehyde, stained with hematoxylin, photographed, and quantified by enumerating the number of cells in five randomly selected fields at a magnification of 200×.

Terminal deoxynucleotidyl transferase-mediated dUTP

nick-end labeling (TUNEL) kit (Roche, Basel, Switzerland) were used to evaluate cell apoptosis. In brief, the TUNEL assay results were observed using fluorescence microscopy (Olympus BX53, Japan), with TUNEL-positive nuclei appearing red in the fluorescence images. The apoptotic rate was determined by calculating the proportion of TUNEL-positive cells per field using Image-Pro Plus software.

Luciferase reporter assays

Wild-type (WT) or mutant-type (Mut) OIP5-AS1 was inserted into the pMIR-REPORT vector (Ambion, Thermo Fisher Scientific, MA, USA). These constructs were then co-transfected with miR-Con or miR-455-3p mimics into the SW1736 and CAL62 cells. Luciferase activity was quantified using dual-luciferase[®] reporter assay system (Promega, Madison, WI, USA).

Bioinformatics analysis

The Cancer Genome Atlas (TCGA) database (<https://www.cancer.gov/ccg/research/genome-sequencing/tcga>) was used to assess data on the expression of MFAP2 and miRs in thyroid carcinoma with the ggplot2 package (version 3.3.3). TargetScan (<http://www.targetscan.org>) was used to predict the MFAP2-related miRs (25). The estimate algorithm was used to analyze the correlation between MFAP2 and the Stromal score, Immune score, and ESTIMATE score, based on data from TCGA database (26). The TIMER database (<http://timer.cistrome.org/>) was used to examine the relationship between MFAP2 and immune infiltration in thyroid carcinoma (27).

Statistical analysis

The data are presented as the mean \pm standard deviation. The statistical analysis was performed using IBM SPSS Statistics Version 19.0 (SPSS Inc., Chicago, IL, USA). The Student's *t*-test or the non-parametric Mann-Whitney test was used to analyze two-group differences. The Wilcoxon paired *t*-test was used to evaluate MFAP2, miR-455-3p, or OIP5-AS1 expression in the thyroid carcinoma tissues and para-carcinoma non-tumor tissues. Inter-group differences were analyzed by a one-way analysis of variance. Spearman's rank analysis was used to identify the correlations. A *P* value <0.05 indicated a statistically significant difference.

Results

MFAP2 expression in pan-cancer and thyroid carcinoma

TCGA database was used to analyze the expression of MFAP2 in pan-cancer. As *Figure 1A* shows, compared to the non-tumor tissues, there was a notable increase in the expression of MFAP2 in 15 types of cancer, but there was only a significant decrease in MFAP2 expression in four types of cancer. The expression of MFAP2 was significantly higher in the thyroid carcinoma tissues than the non-tumor tissues in TCGA and GTEx databases (*Figure 1B*). The expression of MFAP2 was more upregulated in the thyroid carcinoma tissues than the non-tumor tissues in both the unpaired (*Figure 1C*) and paired (*Figure 1D*) samples.

MFAP2 was upregulated in thyroid carcinoma tissues

To confirm the role of MFAP2 in the progression of thyroid carcinoma, the expression of MFAP2 was assessed in matched thyroid carcinoma tissues and cell lines using immunostaining and a RT-qPCR analysis. The IHC staining and RT-qPCR results confirmed that MFAP2 expression was elevated in thyroid carcinoma tissues (*Figure 2A,2B*). In addition, the RT-qPCR analysis revealed that MFAP2 expression was more elevated in the thyroid carcinoma cell lines than the Nthy-ori3-1 cell line (*Figure 2C*).

MFAP2 silencing suppressed the malignant characteristics of thyroid carcinoma cells

In vitro, cell proliferation was significantly inhibited after the transfection of the CAL62 and SW1736 cells with sh-MFAP2, a specific shRNA, for 48 and 72 hours (*Figure 3A,3B*). The transwell assays demonstrated that the introduction of sh-MFAP2 resulted in a notable suppression of thyroid carcinoma cell migration (*Figure 3C*). The TUNEL staining also showed that transfection with sh-MFAP2 elevated the apoptotic cell proportion of thyroid carcinoma cells *in vitro* (*Figure 3D*).

Correlation between MFAP2 and immune infiltration in thyroid carcinoma

As mentioned above, MFAP2 plays a crucial role in the advancement of thyroid carcinoma. Previous studies have shown that immune infiltration in the tumor microenvironment of thyroid carcinoma is correlated with

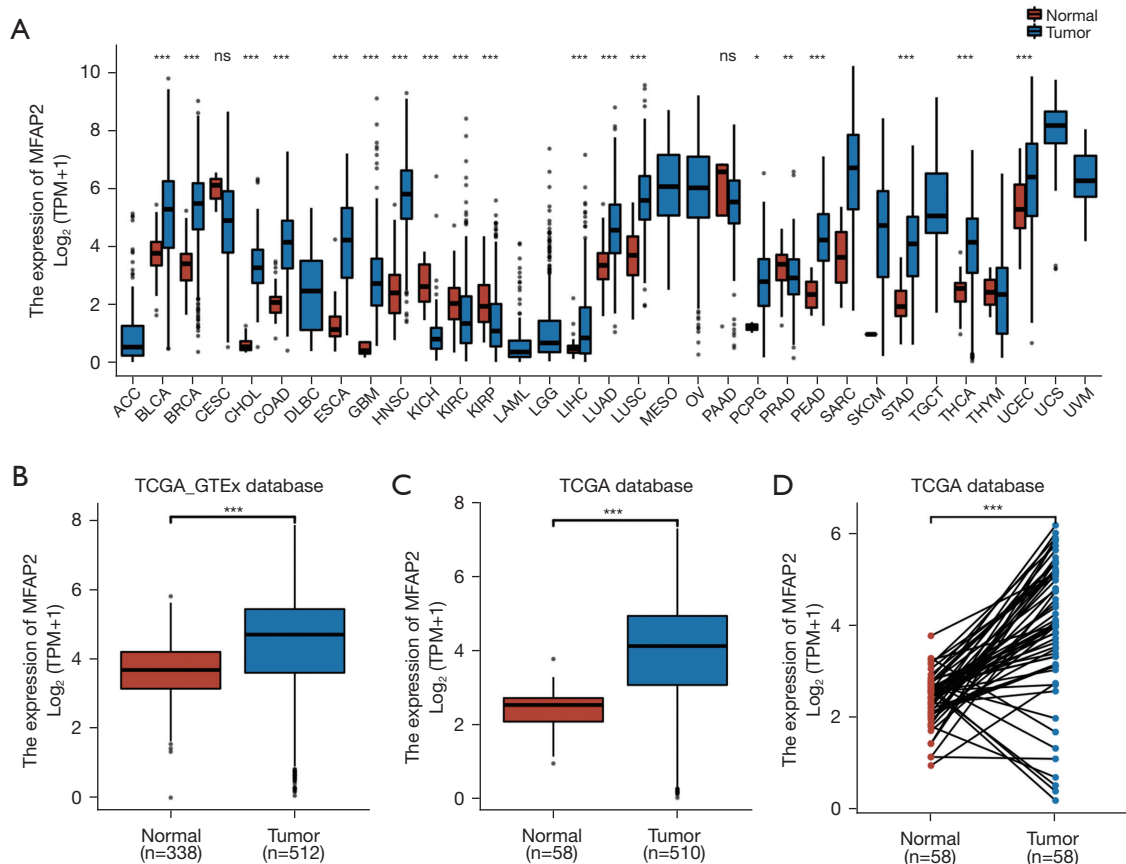


Figure 1 MFAP2 expression in pan-cancer and thyroid carcinoma. TCGA database was used to analyze MFAP2 expression in pan-cancer (A). The analysis of MFAP2 expression in the thyroid carcinoma tissues and non-tumor tissues (B) was performed using TCGA and GTEEx databases. According to TCGA database, MFAP2 was present in both the unpaired (C) and paired (D) tissues. *, $P < 0.05$; **, $P < 0.05$; ***, $P < 0.001$ represents tumor group as compared to normal group. ns, no significant; MFAP2, microfibril-associated protein 2; TPM, transcript per million; TCGA, The Cancer Genome Atlas; GTEEx, Genotype-Tissue Expression.

tumor escape and recurrence (28,29). The role of MFAP2 in the enrichment of immune cells was analyzed using the TIMER database to investigate its association with immune infiltration in thyroid carcinoma. As *Figure 4A* shows, the deletion of MFAP2 at the arm level resulted in a notable reduction in the number of cluster of differentiation (CD) 4^+ T cells in thyroid carcinoma. However, altering the copy number of MFAP2 did not appear to have any discernible effect on the abundance of B cells, CD 8^+ T cells, macrophages, neutrophils, and dendritic cells. As *Figure 4B* shows, there was a strong association between MFAP2 expression and B cells ($r=0.302$, $P < 0.001$), neutrophils ($r=0.290$, $P < 0.001$), dendritic cells ($r=0.319$, $P < 0.001$), and CD 4^+ T cells ($r=0.254$, $P < 0.001$). Using the estimate algorithm (*Figure 4C*) in TCGA database, we found a strong correlation between MFAP2 expression and Stromal score

($r=0.330$, $P < 0.001$), Immune score ($r=0.200$, $P < 0.001$), and ESTIMATE score ($r=0.267$, $P < 0.001$).

Correlation between MFAP2 and immune checkpoint molecules in thyroid carcinoma

Using the TIMER database, we also discovered a significant correlation between the following six immune checkpoint molecules and MFAP2 expression in thyroid carcinoma: programmed cell death 1 (PDCD1) ($r=0.151$, $P < 0.001$; *Figure 5A*), cytotoxic T lymphocyte-associated protein 4 (CTLA4) ($r=0.267$, $P < 0.001$; *Figure 5B*), tumor necrosis factor receptor superfamily member 5 (TNFRSF5, also known as CD40) ($r=0.429$, $P < 0.001$; *Figure 5C*), TNFRSF18 ($r=0.444$, $P < 0.001$; *Figure 5D*), TNFSF18 ($r=0.300$, $P < 0.001$; *Figure 5E*), and butyrophilin 2A1 (BTN2A1)

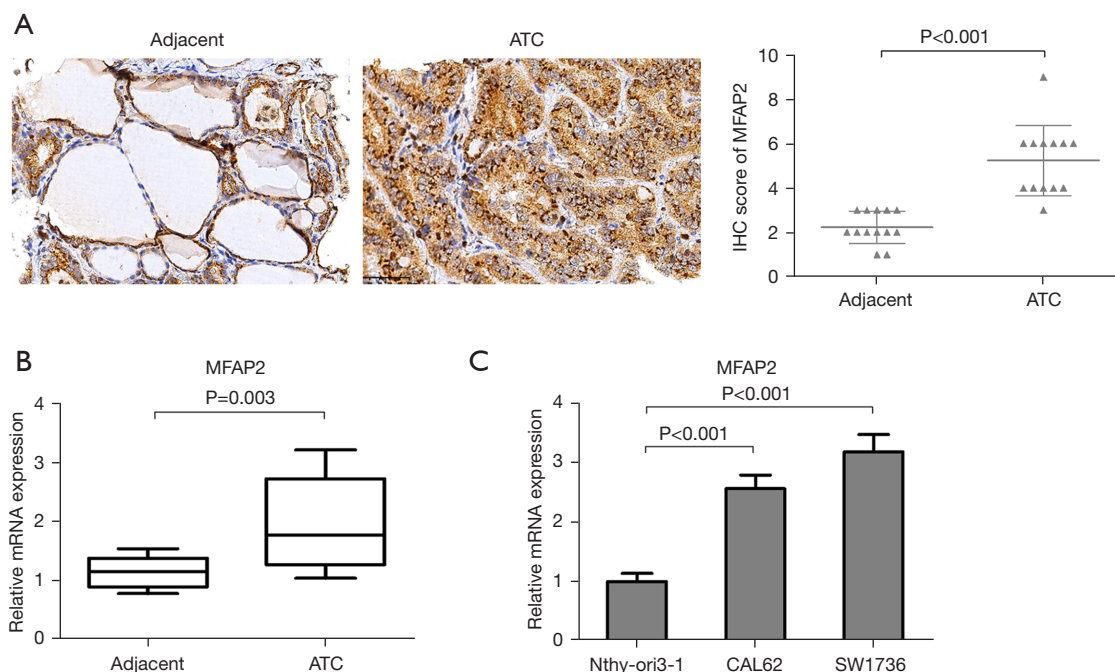


Figure 2 MFAP2 was observed to be upregulated in thyroid carcinoma tissues. Immunostaining was performed to assess MFAP2 expression in 13 pairs of thyroid carcinoma tissues and their corresponding adjacent non-tumor tissues (A) (magnification: 1,000 \times ; scale bar =50 μ m). A RT-qPCR analysis was performed to detect MFAP2 expression in the 13 pairs of thyroid carcinoma tissues and adjacent non-tumor tissues (B) and thyroid carcinoma cell lines (C). ATC, anaplastic thyroid carcinoma; IHC, immunohistochemistry; MFAP2, microfibril-associated protein 2; RT-qPCR, real-time quantitative polymerase chain reaction.

($r=0.260$, $P<0.001$; *Figure 5F*).

MFAP2-related miRs

Using the TargetScan database, we identified nine conserved sites in the 3'-untranslated region of MFAP2 that were predicted to bind with 9 miRs (i.e., hsa-miR-29a-3p, hsa-miR-29c-3p, hsa-miR-29b-3p, hsa-miR-6835-3p, hsa-miR-455-3p, hsa-miR-3184-5p, hsa-miR-423-5p, hsa-miR-140-3p, and hsa-miR-194-5p) (*Figure 6A*). Using TCGA database, we found that hsa-miR-29c-3p (*Figure 6B*), hsa-miR-455-3p (*Figure 6C*), hsa-miR-423-5p (*Figure 6D*), hsa-miR-140-3p (*Figure 6E*), and hsa-miR-194-5p (*Figure 6F*) were significantly more downregulated in the thyroid carcinoma than the non-tumor tissues.

miR-455-3p directly targeted MFAP2 and inhibited thyroid carcinoma cell proliferation *in vitro*

To investigate the regulatory mechanism of thyroid carcinoma progression at the post-transcriptional level,

we identified MFAP2 as a potential target of miR-455-3p using a bioinformatics algorithm (*Figure 7A*). The luciferase activity in the WT-type cells was significantly reduced following transfection with miR-455-3p mimics, but no change was observed in the Mut-type cells (*Figure 7B*). This indicated that miR-455-3p had the ability to directly target MFAP2 in the CAL62 and SW1736 cells. Further, a western blot analysis was performed to investigate whether miR-455-3p was involved in the post-transcriptional translation of MFAP2. Following the introduction of miR-455-3p mimics into the CAL62 and SW1736 cells, the expression of the MFAP2 protein was notably diminished compared to that of the control group (*Figure 7C*). The RT-qPCR results showed that miR-455-3p was significantly decreased in the thyroid carcinoma tissues compared to the surrounding non-tumor tissues (*Figure 7D*). Experimental measurements conducted *in vitro* demonstrated that the introduction of miR-455-3p mimics hampered the growth of cells (*Figure 7E*) and their migration (*Figure 7F*), but enhanced the percentage of TUNEL positive staining cells (*Figure 7G*).

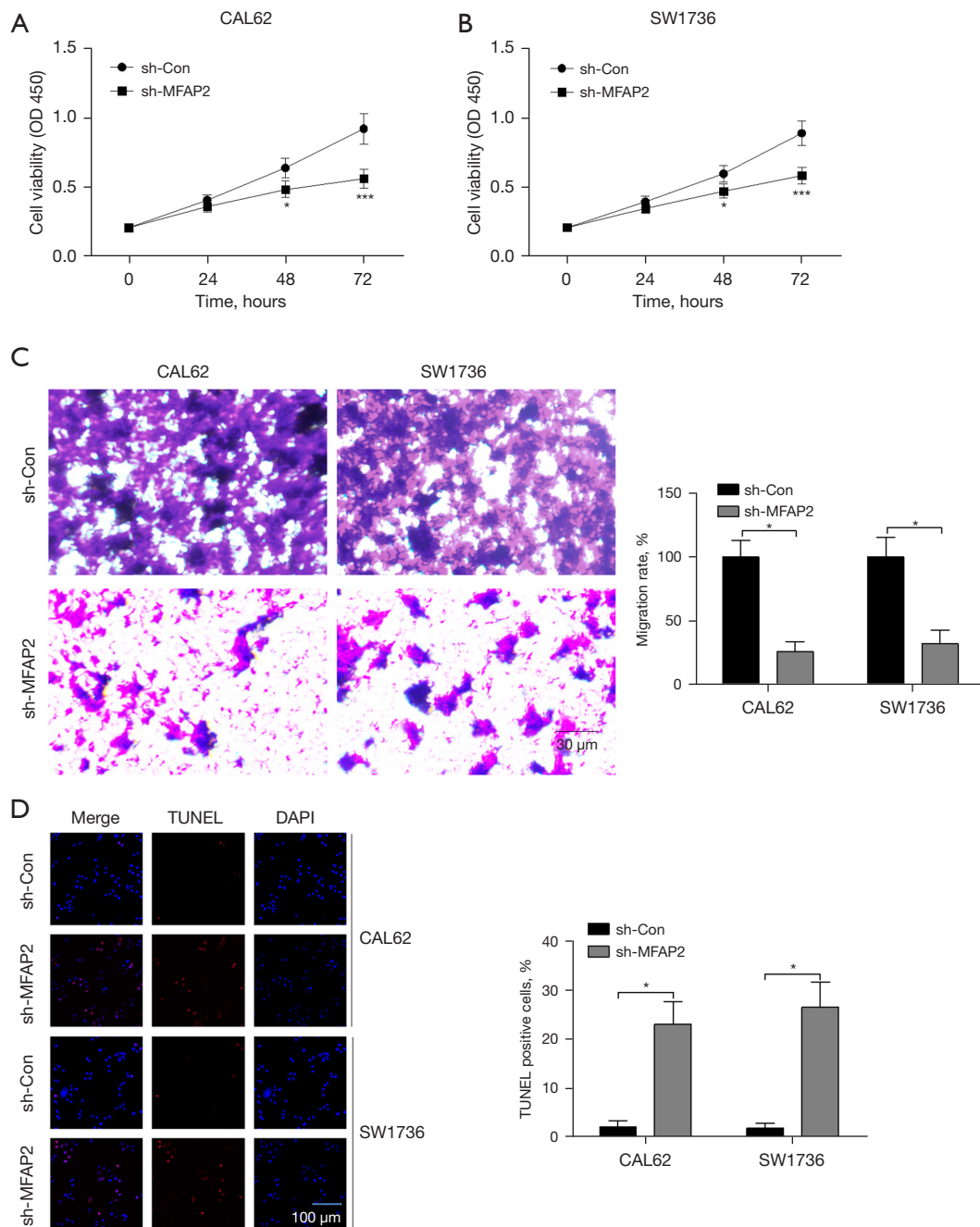


Figure 3 The silencing of MFAP2 inhibited the malignant phenotype of the thyroid carcinoma cells *in vitro*. After transfection with sh-Con or sh-MFAP2 into the CAL62 and SW1736 cells, cell proliferation (A,B), migration (C), and apoptosis (D) were detected using CCK-8, transwell migration assay without matrigel by crystal violet staining, and TUNEL assays, respectively. *, $P < 0.05$; ***, $P < 0.001$ compared with the corresponding control group. Triplicate repetitions were performed in each group. OD, optical density; MFAP2, microfibril-associated protein 2; TUNEL, terminal deoxynucleotidyl transferase-mediated dUTP nick-end labeling; DAPI, 4',6-diamidino-2-phenylindole; CCK-8, Cell Counting Kit-8.

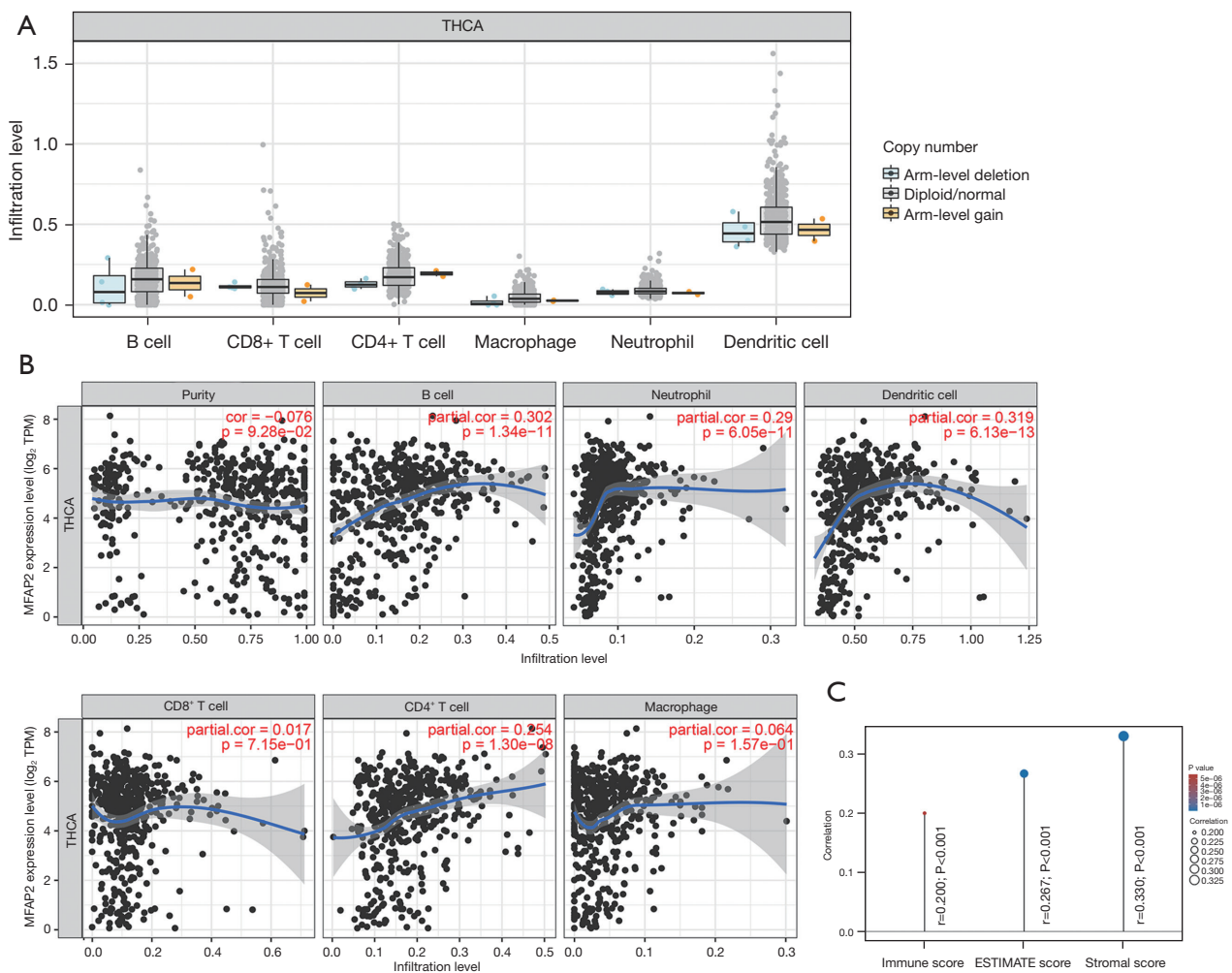


Figure 4 The correlation between MFAP2 and immune infiltration in thyroid carcinoma. The TIMER database was used to analyze the role of MFAP2 copy number in the enrichment of the immune cells (A). The TIMER database was also used to evaluate the association between MFAP2 and immune cell enrichment (B). Using TCGA database, an estimate algorithm was used to analyze the correlation between MFAP2 and the Stromal score, Immune score, and ESTIMATE score (C). THCA, thyroid carcinoma; MFAP2, microfibril-associated protein 2; TPM, transcript per million; TIMER, tumor immune estimation resource; TCGA, The Cancer Genome Atlas.

OIP5-AS1 mediated the expression of miR-455-3p/ MFAP2 axis

Based on LncBase Predicted v.3 of DIANA tools (<https://diana.e-ce.uth.gr/lncbasev3>), miR-455-3p was identified as a possible candidate for targeting by OIP5-AS1 (Figure 8A). According to the luciferase analysis, the introduction of miR-455-3p decreased luciferase activity in the CAL62 cells with the WT OIP5-AS1. However, it had no effect on luciferase activity in the CAL62 cells with the Mut-OIP5-AS1 (Figure 8A). Further, the expression of OIP5-AS1 was markedly elevated in the thyroid carcinoma tissues

(Figure 8B) and cell lines (Figure 8C) compared to the corresponding normal non-tumor tissues or cells. We also examined whether miR-455-3p was a direct recipient of OIP5-AS1. In two separate thyroid carcinoma cell lines, the OIP5-AS1 gene was silenced. Following the introduction of sh-OIP5-AS1 into the CAL62 and SW1736 cells, the expression of OIP5-AS1 was reduced by around 70% (Figure 8D). Transfection with sh-OIP5-AS1 resulted in the upregulation of miR-455-3p (Figure 8E) and the downregulation of MFAP2 (Figure 8F) in both the CAL62 and SW1736 cells. These findings suggest that OIP5-AS1 is capable of directly controlling the expression of miR-455-

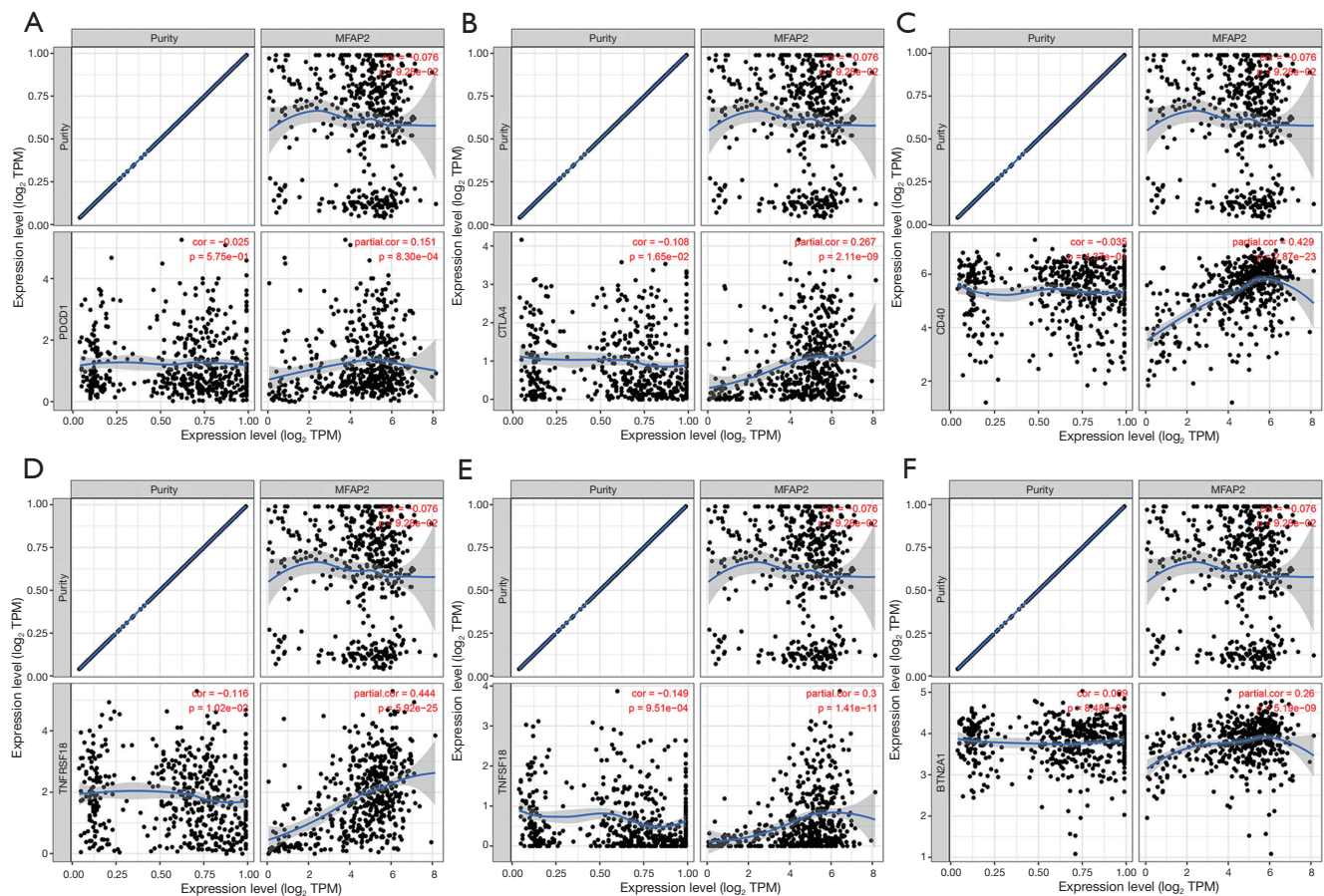


Figure 5 The correlation between MFAP2 and immune checkpoint molecules in thyroid carcinoma. The TIMER database was used to analyze the correlation between MFAP2 and PDCD1 (A), CTLA4 (B), CD40 (C), TNFRSF18 (D), TNFSF18 (E), and BTN2A1 (F) in thyroid carcinoma. TPM, transcript per million; MFAP2, microfibril-associated protein 2; PDCD1, programmed cell death protein 1; CTLA4, cytotoxic T lymphocyte-associated antigen-4; CD40, tumor necrosis factor receptor superfamily member 5; TNFRSF18, tumor necrosis factor receptor superfamily member 18; TNFSF18, tumor necrosis factor superfamily member 18; BTN2A1, butyrophilin subfamily 2 member A1.

3p and MFAP2. Further, a negative association was found between the levels of OIP5-AS1 and miR-455-3p ($r=-0.704$; $P=0.007$; *Figure 8G*), while a positive association was found between the expression of OIP5-AS1 and MFAP2 in the thyroid carcinoma tissues ($r=0.563$; $P=0.045$; *Figure 8H*). A negative relationship between the levels of miR-455-3p and MFAP2 expression was also confirmed in the thyroid carcinoma tissues ($r=-0.672$; $P=0.01$; *Figure 8I*).

The antineoplastic activities of the sh-OIP5-AS1 and miR-455-3p mimics were reversed by MFAP2 overexpression

To further investigate the association between OIP5-AS1 and MFAP2, as well as miR-455-3p and MFAP2, we co-

expressed sh-OIP5-AS1 and MFAP2, or we simultaneously introduced miR-455-3p mimics and MFAP2 into the CAL62 and SW1736 cells. The growth inhibition induced by the transfection of sh-OIP5-AS1 or miR-455-3p mimics was reversed by the overexpression of the MFAP2 plasmids (*Figure 9A,9B*). Additionally, MFAP2 overexpression neutralized migration inhibition in the sh-OIP5-AS1 or miR-455-3p mimic-transfected cells (*Figure 9C,9D*). Further, the induction of apoptosis by the sh-OIP5-AS1 or miR-455-3p mimics was reduced when the CAL62 and SW1736 cells were transfected with plasmids overexpressing MFAP2 (*Figure 9E,9F*). The results suggest that the OIP5-AS1/miR-455-3p/MFAP2 axis plays a role in the advancement of thyroid carcinoma.

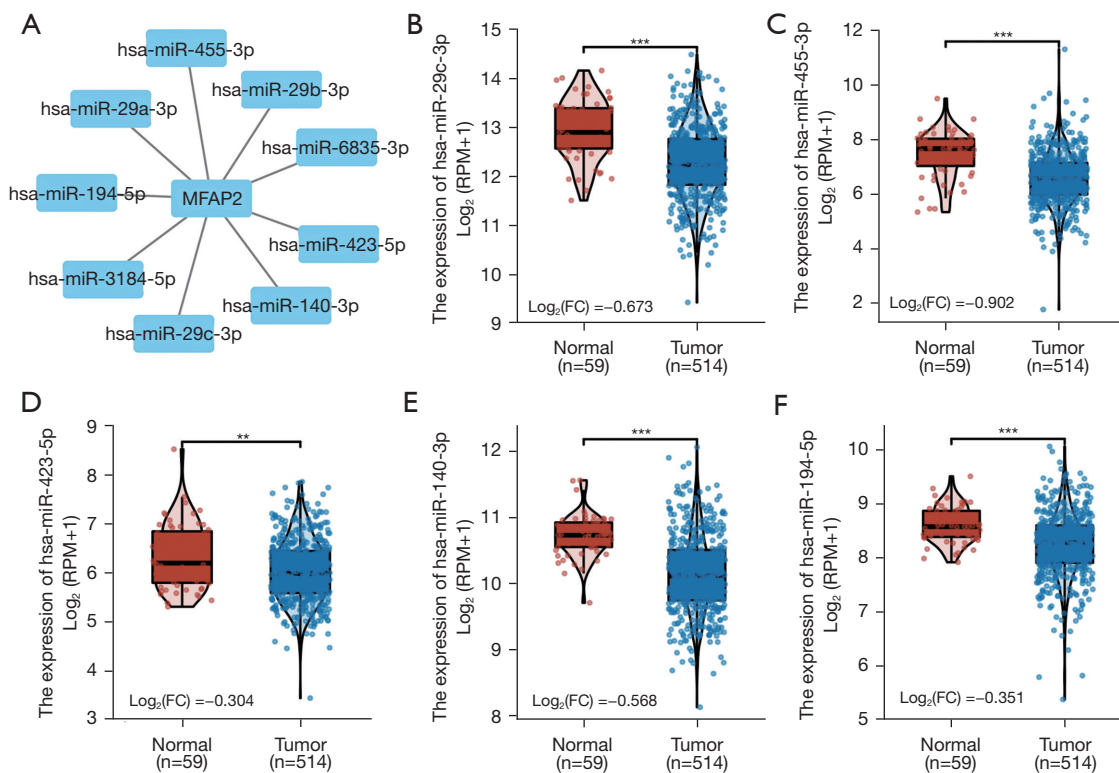


Figure 6 MFAP2-related miRs. The TargetScan database was used to predict the conserved sites in the 3'-untranslated region of MFAP2 and the miRs (A). TCGA database was used to analyze the expression of hsa-miR-29c-3p (B), hsa-miR-455-3p (C), hsa-miR-423-5p (D), hsa-miR-140-3p (E), and hsa-miR-194-5p (F) in the thyroid carcinoma tissues compared with the non-tumor tissues. **, $P < 0.05$; ***, $P < 0.001$ represents tumor group as compared to normal group. RPM, transcript per million; FC, fold change; MFAP2, microfibril-associated protein 2; TCGA, The Cancer Genome Atlas.

Discussion

Our research primarily concentrated on the fundamental regulatory mechanism of lncRNAs acting as ceRNAs to sequester miRNAs and facilitate the modulation of their subsequent target gene expression. Our findings indicate that the expression of OIP5-AS1 is elevated in both thyroid carcinoma tissues and cell lines. In thyroid carcinoma tissues, we observed an increase in MFAP2 expression and a decrease in miR-455-3p levels. Following transfection with sh-OIP5-AS1, the CAL62 and SW1736 cells exhibited an increase in miR-455-3p expression and a decrease in MFAP2 expression in the *in vitro* transfection experiment. The suppression of OIP5-AS1 enhanced cellular apoptosis and impaired cellular proliferation and migration in the CAL62 and SW1736 cells. The *in vitro* experiments showed that both the suppression of MFAP2 and the increased expression of miR-455-3p exerted significant anti-cancer effects. Interestingly, the overexpression of MFAP2

counteracted the anti-cancer effects of the sh-OIP5-AS1 and miR-455-3p mimics when tested in a laboratory setting. In the CAL62 and SW1736 cells, OIP5-AS1 acted as a ceRNA to suppress the expression of miR-455-3p and enhance the expression of MFAP2, which is a direct target of miR-455-3p.

OIP5-AS1 is abnormally expressed in more than 10 cancer types and is associated with various cellular processes, including cell growth, invasion, movement, cell death, cell division, and EMT (18,30-32). However, OIP5-AS1 has a dual function as both an oncogene and a tumor suppressor in different types of malignant tumors (30,31). For example, OIP5-AS1 downregulation, which promotes cell proliferation through the upregulation of miR-410, has been confirmed in cases of multiple myeloma (30). Conversely, OIP5-AS1 is more highly expressed in pancreatic cancer tissues than non-tumor tissues (31). The inhibition of OIP5-AS1 hampers cellular

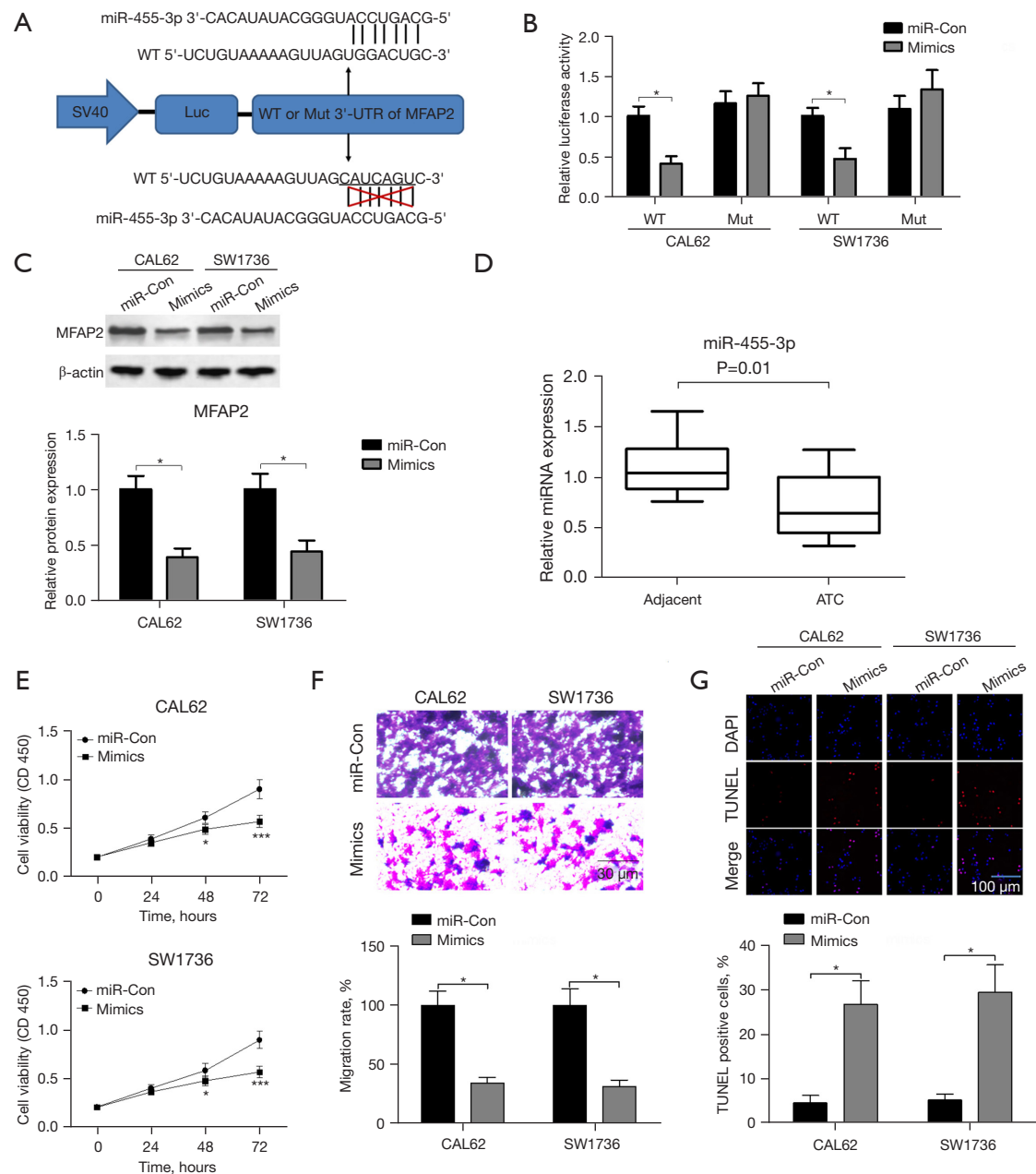


Figure 7 miR-455-3p directly targets MFAP2 and inhibits thyroid carcinoma cell proliferation *in vitro*. On-line bioinformatics software Targetscan (<http://www.targetscan.org>) and DIANA (<http://www.microrna.gr/microT-CDS>) were used to predict the binding sites between miR-455-3p and MFAP2 (A). Dual-luciferase[®] reporter assay system was performed to evaluate the direct association between miR-455-3p and MFAP2 (B). After transfection with miR-455-3p mimics into the CAL62 and SW1736 cells, western blot was used to measure MFAP2 protein expression (C). RT-qPCR assays were used to measure miR-455-3p expression in the thyroid carcinoma tissues and adjacent non-tumor tissues (D). After transfection with miR-455-3p mimics into the CAL62 and SW1736 cells, cell proliferation (E), migration (F), and apoptosis (G) were detected using CCK-8, transwell migration assay without matrigel by crystal violet staining, and TUNEL assays, respectively. *, $P < 0.05$; ***, $P < 0.001$ compared with the corresponding control group. miR-Con, microRNA control; WT, wild type; Mut, mutant; OD, optical density; TUNEL, terminal deoxynucleotidyl transferase-mediated dUTP nick-end labeling; DAPI, 4',6-diamidino-2-phenylindole; MFAP2, microfibril-associated protein 2; RT-qPCR, real-time quantitative polymerase chain reaction; CCK-8, Cell Counting Kit-8.

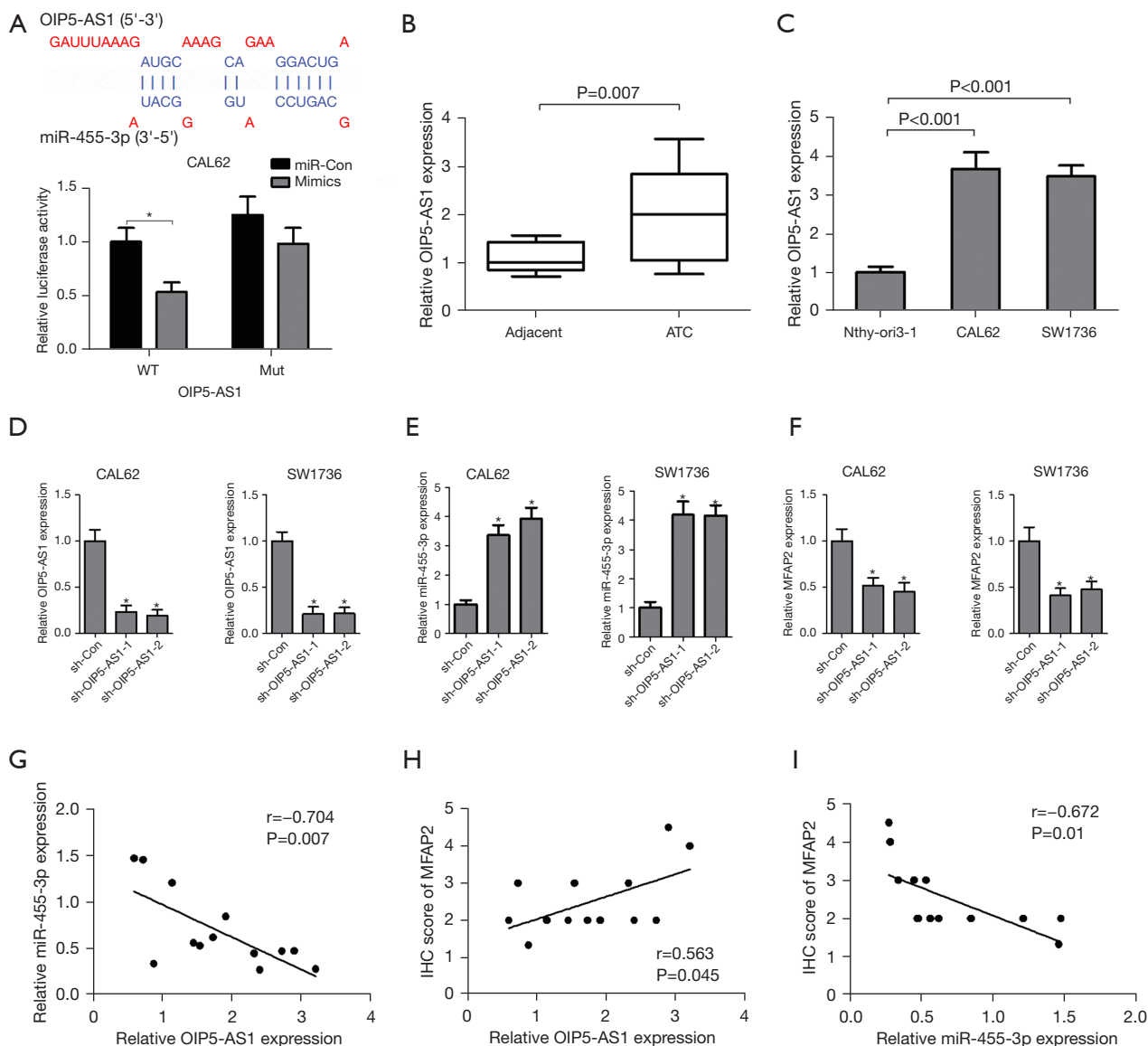


Figure 8 OIP5-AS1 mediated the expression of miR-455-3p/MFAP2 axis. LncBase Predicted v.2 of DIANA tools were used to predict the binding sites between OIP5-AS1 and miR-455-3p (A). RT-qPCR was used to measure OIP5-AS1 expression in the thyroid carcinoma tissues (B) and cell lines (C). After transfection with sh-OIP5-AS1 into the CAL62 and SW1736 cells, RT-qPCR assays were used to detect OIP5-AS1 (D), miR-455-3p (E), and MFAP2 (F). A Pearson correlation analysis was performed to evaluate the association between OIP5-AS1 and miR-455-3p (G), OIP5-AS1 and MFAP2 (H), or miR-455-3p and MFAP2 (I) in the thyroid carcinoma tissues. *, P<0.05 compared with the corresponding control group. miR-Con, microRNA control; WT, wild type; Mut, mutant; OIP5-AS1, opa interacting protein 5-antisense RNA 1; ATC, anaplastic thyroid carcinoma; sh-Con, short hairpin RNA control; MFAP2, microfibril-associated protein 2; RT-qPCR, real-time quantitative polymerase chain reaction.

proliferation and triggers cell cycle cessation in pancreatic cancer cells (31). OIP5-AS1 has been shown to be substantially elevated in both thyroid cancer tumor tissues and cell lines, and can serve as a prognostic indicator for

unfavorable outcomes (22). The suppression of OIP5-AS1 hampers the proliferation and migration of cells, while the upregulation of OIP5-AS1 enhances the proliferative and migratory abilities of TPC-1 and BCPAP cells (22).

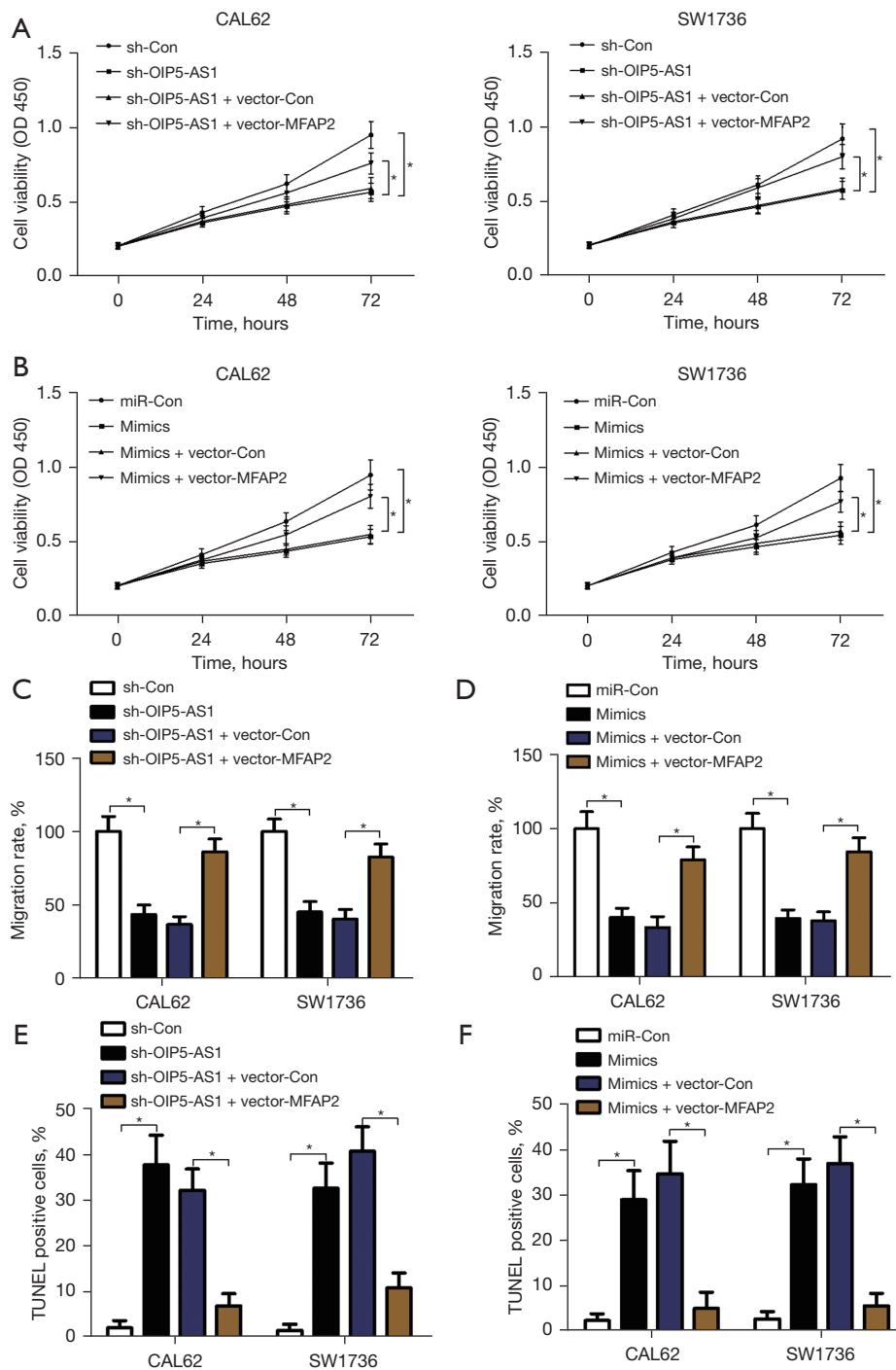


Figure 9 The overexpression of MFAP2 reversed the antineoplastic activities of the sh-OIP5-AS1 and miR-455-3p mimics *in vitro*. Cell proliferation (A), migration (C), and apoptosis (E) were assessed in the CAL62 and SW1736 cells after co-transfection with the sh-OIP5-AS1 and MFAP2 overexpressed plasmids using CCK-8, transwell, and TUNEL assays, respectively. Cell proliferation (B), migration (D), and apoptosis (F) were detected in the CAL62 and SW1736 cells after co-transfection with the miR-455-3p mimics and MFAP2 overexpressed plasmids using CCK-8, transwell, and TUNEL assays, respectively. *, $P < 0.05$ compared with the corresponding control group. OD, optical density; sh-Con, short hairpin RNA control; OIP5-AS1, opa interacting protein 5-antisense RNA 1; miR-Con, microRNA control; TUNEL, terminal deoxynucleotidyl transferase-mediated dUTP nick-end labeling; MFAP2, microfibril-associated protein 2; CCK-8, Cell Counting Kit-8.

Our study also confirmed that OIP5-AS1 expression was notably increased in thyroid carcinoma tissues and cell lines compared to the respective control tissues. Functional assays conducted *in vitro* demonstrated that the depletion of OIP5-AS1 hindered the growth and movement of the CAL62 and SW1736 cells, while promoting their apoptosis. These findings suggest that inhibiting OIP5-AS1 may be a viable therapeutic approach for impeding the advancement of thyroid carcinoma.

To date, most research has focused on OIP5-AS1 as a decoy for sponging numerous miRs to regulate protein translation in multiple malignant tumors (18,33). For instance, Tao *et al.* discovered that OIP5-AS1, as a ceRNA, promotes gastric cancer progression by abrogating miR-367-3p-mediated high mobility group A2 repression (34). In our study, miR-455-3p was shown to be a direct target of OIP5-AS1. The knockdown of OIP5-AS1 led to the accumulation of miR-455-3p that inhibited cell proliferation and migration, and evoked cell apoptosis in the CAL62 and SW1736 cells.

Emerging evidence indicates that MFAP2 is upregulated in multiple cancers, including gastric cancer, hepatocellular carcinoma, and breast cancer (7,9,10). Using TCGA data set, Dong *et al.* (35) reported that MFAP2 expression is significantly higher in papillary thyroid cancer tissues than normal non-tumor tissues. Additionally, when BCPAP and TPC-1 cell lines were transfected with small-interfering RNA to suppress MFAP2 expression, an increase in apoptotic proportion and a decrease in cell viability, migration, and invasion were observed (35). Notably, our research indicated that the expression of MFAP2 is increased in thyroid carcinoma tissues and cell lines. Additionally, suppressing MFAP2 resulted in a substantial reduction in cell proliferation and migration, while promoting cell apoptosis in the CAL62 and SW1736 cells. Further, the overabundance of MFAP2 nullified the physiological effects of sh-OIP5-AS1 or miR-455-3p in the CAL62 and SW1736 cells. Further, the correlation between MFAP2 expression and the enrichment of various immune cells and immune checkpoint molecules implies that targeting MFAP2 could potentially improve the effectiveness of immunotherapy in thyroid carcinoma.

Currently, the primary constraint impeding the clinical utilization of lncRNA is the delivery technology. It is well established that small nucleic acid drugs are extensively employed in clinical practice, with a predominant focus on intrahepatic or hepatic metabolism diseases utilizing GalNAc targeting technology (36,37). Targeting tissues

outside of the liver has historically posed challenges in clinical treatment. However, advancements in scientific research, particularly in the development of lipid nanoparticle (LNP) technology, have offered promising solutions to enhance the delivery of nucleic acid drugs to these tissues despite their large molecular weight (38). Consequently, the primary barriers hindering the clinical application of lncRNA, small interfering RNA, and microRNA are predominantly attributed to limitations in delivery technology. Addressing these challenges holds the potential to significantly advance the utilization of nucleic acid drugs in clinical settings.

Conclusions

OIP5-AS1 plays a role in the progression of thyroid carcinoma through the mediation of the miR-455-3p/MFAP2 signaling axis. The OIP5-AS1/miR-455-3p/MFAP2 signal transduction pathway provides a theoretical foundation for clinical therapies for thyroid carcinoma.

Acknowledgments

Funding: This work was supported by funding from the Natural Science Foundation in the Xinjiang Uygur Autonomous Region (No. 2023D01C59).

Footnote

Reporting Checklist: The authors have completed the MDAR reporting checklist. Available at <https://tcr.amegroups.com/article/view/10.21037/tcr-24-630/rc>

Data Sharing Statement: Available at <https://tcr.amegroups.com/article/view/10.21037/tcr-24-630/dss>

Peer Review File: Available at <https://tcr.amegroups.com/article/view/10.21037/tcr-24-630/prf>

Conflicts of Interest: All authors have completed the ICMJE uniform disclosure form (available at <https://tcr.amegroups.com/article/view/10.21037/tcr-24-630/coif>). The authors have no conflicts of interest to declare.

Ethical Statement: The authors are accountable for all aspects of the work in ensuring that questions related to the accuracy or integrity of any part of the work are appropriately investigated and resolved. The study was

approved by the Ethics Committee of the People's Hospital of Xinjiang Uygur Autonomous Region (approval number: 20210345). Informed consent forms were signed by the thyroid carcinoma patients before sample collection. The study conformed to the provisions of the Declaration of Helsinki (as revised in 2013).

Open Access Statement: This is an Open Access article distributed in accordance with the Creative Commons Attribution-NonCommercial-NoDerivs 4.0 International License (CC BY-NC-ND 4.0), which permits the non-commercial replication and distribution of the article with the strict proviso that no changes or edits are made and the original work is properly cited (including links to both the formal publication through the relevant DOI and the license). See: <https://creativecommons.org/licenses/by-nc-nd/4.0/>.

References

- Xue M, Mi S, Zhang Z, et al. MFAP2, upregulated by m1A methylation, promotes colorectal cancer invasiveness via CLK3. *Cancer Med* 2023;12:8403-14.
- Wei R, Song J, Liu X, et al. Immunosuppressive MFAP2(+) cancer associated fibroblasts conferred unfavorable prognosis and therapeutic resistance in gastric cancer. *Cell Oncol (Dordr)* 2024;47:55-68.
- Turecamo SE, Walji TA, Broekelmann TJ, et al. Contribution of metabolic disease to bone fragility in MAGP1-deficient mice. *Matrix Biol* 2018;67:1-14.
- Zhu S, Ye L, Bennett S, et al. Molecular structure and function of microfibrillar-associated proteins in skeletal and metabolic disorders and cancers. *J Cell Physiol* 2021;236:41-8.
- Walji TA, Turecamo SE, Sanchez AC, et al. Marrow Adipose Tissue Expansion Coincides with Insulin Resistance in MAGP1-Deficient Mice. *Front Endocrinol (Lausanne)* 2016;7:87.
- Alonso F, Dong Y, Li L, et al. Fibrillin-1 regulates endothelial sprouting during angiogenesis. *Proc Natl Acad Sci U S A* 2023;120:e2221742120.
- Yao LW, Wu LL, Zhang LH, et al. MFAP2 is overexpressed in gastric cancer and promotes motility via the MFAP2/integrin $\alpha 5\beta 1$ /FAK/ERK pathway. *Oncogenesis* 2020;9:17.
- Wang JK, Wang WJ, Cai HY, et al. MFAP2 promotes epithelial-mesenchymal transition in gastric cancer cells by activating TGF- β /SMAD2/3 signaling pathway. *Onco Targets Ther* 2018;11:4001-17.
- Zhu X, Cheng Y, Wu F, et al. MFAP2 Promotes the Proliferation of Cancer Cells and Is Associated With a Poor Prognosis in Hepatocellular Carcinoma. *Technol Cancer Res Treat* 2020;19:1533033820977524.
- Gong X, Dong T, Niu M, et al. lncRNA LCPAT1 Upregulation Promotes Breast Cancer Progression via Enhancing MFAP2 Transcription. *Mol Ther Nucleic Acids* 2020;21:804-13.
- Chen Z, Lv Y, Cao D, et al. Microfibril-Associated Protein 2 (MFAP2) Potentiates Invasion and Migration of Melanoma by EMT and Wnt/ β -Catenin Pathway. *Med Sci Monit* 2020;26:e923808.
- Shabna A, Bindhya S, Sidhanth C, et al. Long non-coding RNAs: Fundamental regulators and emerging targets of cancer stem cells. *Biochim Biophys Acta Rev Cancer* 2023;1878:188899.
- Nemeth K, Bayraktar R, Ferracin M, et al. Non-coding RNAs in disease: from mechanisms to therapeutics. *Nat Rev Genet* 2024;25:211-32.
- Luo Y, Ye Y, Zhang Y, et al. New insights into COL26A1 in thyroid carcinoma: prognostic prediction, functional characterization, immunological drug target and ceRNA network. *Transl Cancer Res* 2023;12:3384-408.
- Wang Y, Hardin H, Chu YH, et al. Long Non-coding RNA Expression in Anaplastic Thyroid Carcinomas. *Endocr Pathol* 2019;30:262-9.
- Wang XM, Liu Y, Fan YX, et al. lncRNA PTCSC3 affects drug resistance of anaplastic thyroid cancer through STAT3/INO80 pathway. *Cancer Biol Ther* 2018;19:590-7.
- Zhang R, Hardin H, Huang W, et al. MALAT1 Long Non-coding RNA Expression in Thyroid Tissues: Analysis by In Situ Hybridization and Real-Time PCR. *Endocr Pathol* 2017;28:7-12.
- Li Y, Han X, Feng H, et al. Long noncoding RNA OIP5-AS1 in cancer. *Clin Chim Acta* 2019;499:75-80.
- Zou Y, Yao S, Chen X, et al. lncRNA OIP5-AS1 regulates radioresistance by targeting DYRK1A through miR-369-3p in colorectal cancer cells. *Eur J Cell Biol* 2018;97:369-78.
- Kun-Peng Z, Chun-Lin Z, Xiao-Long M, et al. Fibronectin-1 modulated by the long noncoding RNA OIP5-AS1/miR-200b-3p axis contributes to doxorubicin resistance of osteosarcoma cells. *J Cell Physiol* 2019;234:6927-39.
- Luan W, Zhang X, Ruan H, et al. Long noncoding RNA OIP5-AS1 acts as a competing endogenous RNA to promote glutamine catabolism and malignant melanoma growth by sponging miR-217. *J Cell Physiol*

- 2019;234:16609-18.
22. Li Q, Chen W, Luo R, et al. Upregulation of OIP5-AS1 Predicts Poor Prognosis and Contributes to Thyroid Cancer Cell Proliferation and Migration. *Mol Ther Nucleic Acids* 2020;20:279-91.
 23. Liu Z, Dou C, Yao B, et al. Ftx non coding RNA-derived miR-545 promotes cell proliferation by targeting RIG-I in hepatocellular carcinoma. *Oncotarget* 2016;7:25350-65.
 24. Ren L, Chen H, Song J, et al. MiR-454-3p-Mediated Wnt/ β -catenin Signaling Antagonists Suppression Promotes Breast Cancer Metastasis. *Theranostics* 2019;9:449-65.
 25. Agarwal V, Bell GW, Nam JW, et al. Predicting effective microRNA target sites in mammalian mRNAs. *Elife* 2015;4:e05005.
 26. Yoshihara K, Shahmoradgoli M, Martínez E, et al. Inferring tumour purity and stromal and immune cell admixture from expression data. *Nat Commun* 2013;4:2612.
 27. Li T, Fu J, Zeng Z, et al. TIMER2.0 for analysis of tumor-infiltrating immune cells. *Nucleic Acids Res* 2020;48:W509-14.
 28. Yang Z, Wei X, Pan Y, et al. A new risk factor indicator for papillary thyroid cancer based on immune infiltration. *Cell Death Dis* 2021;12:51.
 29. Xie Z, Li X, He Y, et al. Immune Cell Confrontation in the Papillary Thyroid Carcinoma Microenvironment. *Front Endocrinol (Lausanne)* 2020;11:570604.
 30. Yang N, Chen J, Zhang H, et al. LncRNA OIP5-AS1 loss-induced microRNA-410 accumulation regulates cell proliferation and apoptosis by targeting KLF10 via activating PTEN/PI3K/AKT pathway in multiple myeloma. *Cell Death Dis* 2017;8:e2975.
 31. Meng X, Ma J, Wang B, et al. Long non-coding RNA OIP5-AS1 promotes pancreatic cancer cell growth through sponging miR-342-3p via AKT/ERK signaling pathway. *J Physiol Biochem* 2020;76:301-15.
 32. Chen J, Wang W, Zhang Y, et al. OIP5-AS1/CD147/TRPM7 axis promotes gastric cancer metastasis by regulating apoptosis related PI3K-Akt signaling. *Front Oncol* 2023;13:1221445.
 33. Liu M, Song X, Sun Y, et al. LncRNA OIP5-AS1 Targets the miR-140-5p/UBR5 Cascade to Promote the Development of Gastric Cancer. *Mol Biotechnol* 2023. [Epub ahead of print]. doi: 10.1007/s12033-023-00958-x.
 34. Tao Y, Wan X, Fan Q, et al. Long non-coding RNA OIP5-AS1 promotes the growth of gastric cancer through the miR-367-3p/HMGA2 axis. *Dig Liver Dis* 2020;52:773-9.
 35. Dong SY, Chen H, Lin LZ, et al. MFAP2 is a Potential Diagnostic and Prognostic Biomarker That Correlates with the Progression of Papillary Thyroid Cancer. *Cancer Manag Res* 2020;12:12557-67.
 36. Ranasinghe P, Addison ML, Dear JW, et al. Small interfering RNA: Discovery, pharmacology and clinical development-An introductory review. *Br J Pharmacol* 2023;180:2697-720.
 37. Won Lee J, Kyu Shim M, Kim H, et al. RNAi therapies: Expanding applications for extrahepatic diseases and overcoming delivery challenges. *Adv Drug Deliv Rev* 2023;201:115073.
 38. Eygeris Y, Gupta M, Kim J, et al. Chemistry of Lipid Nanoparticles for RNA Delivery. *Acc Chem Res* 2022;55:2-12.

Cite this article as: Huang R, Liu H, Wang C. OIP5-AS1/miR-455-3p/microfibril-associated protein 2 axis exacerbates the progression of thyroid carcinoma. *Transl Cancer Res* 2024;13(6):3046-3061. doi: 10.21037/tcr-24-630